NJC

Accepted Manuscript

This is an *Accepted Manuscript*, which has been through the Royal Society of Chemistry peer review process and has been accepted for publication.

Accepted Manuscripts are published online shortly after acceptance, before technical editing, formatting and proof reading. Using this free service, authors can make their results available to the community, in citable form, before we publish the edited article. We will replace this *Accepted Manuscript* with the edited and formatted *Advance Article* as soon as it is available.

You can find more information about *Accepted Manuscripts* in the Information for Authors.

Please note that technical editing may introduce minor changes to the text and/or graphics, which may alter content. The journal's standard Terms & Conditions and the Ethical guidelines still apply. In no event shall the Royal Society of Chemistry be held responsible for any errors or omissions in this *Accepted Manuscript* or any consequences arising from the use of any information it contains.

ROYAL SOCIETY OF CHEMISTRY

www.rsc.org/njc

ARTICLE

Supercapacitive behavior of an asymmetric supercapacitor based on $Ni(OH)_2$/XC-72 composite

Received 00th January 20xx,
Accepted 00th January 20xx

DOI: 10.1039/x0xx00000x

www.rsc.org/

Leping Sui, [ab] Shuihua Tang,*[ab] Zhen Dai,[ac] Zhentao Zhu,[ab] Haixin Huangfu,[ab] Xiaolong Qin,[ab] Yuxiao Deng,[ab] and Geir Martin Haarberg*[d]

$Ni(OH)_2$/Vulcan XC-72 (XC-72) composite has been synthesized by a microwave assisted method, it demonstrated a high specific capacitance of 1560 F g^{-1} at 1 A g^{-1} with carbon nanotubes as a conductive agent. $Ni(OH)_2$/XC-72, activated carbon (AC) and non-woven fabric were respectively used as positive electrode, negative electrode and a separator to assemble an asymmetric supercapacitor. This AC//$Ni(OH)_2$/XC-72 supercapacitor achieves a remarkable capacitance of 92.2 F g^{-1} at current density of 0.5 A g^{-1}, maximum energy density of 36 Wh kg^{-1} and power density of 490 W kg^{-1} based on active material in 6 M KOH aqueous electrolyte with negative/positive electrode mass ratio of 1.75 within a voltage window of 1.6 V. Furthermore, the capacitance of the unit supercapacitor remains 85% after 1000 charging—discharging cycles. These results indicate that the AC//$Ni(OH)_2$/XC-72 supercapacitor is promising to be applied in a practical device for energy storage.

Introduction

As an efficient, clean and sustainable energy device, supercapacitors have attracted significant attention due to their high power density, long cycle life and fast charging-discharging rate. [1,2]Generally, based on its energy storage principles, a supercapacitor can be divided into two types. One is defined as an electrical double layer capacitor (EDLC), electrical energy is electrostatically stored at an interface between a conductive electrode and an electrolyte. The other one is defined as a pseudocapacitor, electrical energy is stored by faradaic reactions such as redox reaction, intercalation, or electrosorption.[3] Generally speaking, carbon materials, like activated carbon,[4] carbon fiber,[5] carbon aerogel,[6] reduced graphene oxide[7] and so on, are widely used as EDLC materials due to their low cost, excellent chemical stability, good electronic conductivity and wide operating window.[8] On the other hand, conducting polymers, transition-metal oxide and hydroxides, such as polyaniline (PANI),[9] polypyrrole (PPy), [10] ppy based composites,[11,12] RuO_2,[13] MnO_2,[14] are mostly investigated as pseudocapacitor materials due to the high theoretical capacitance. However, poor electrical conductivity and narrow working window have limited their development.[15,16] $Ni(OH)_2$ based on composite[17] also showed the high specific capacitance, it is suitable for energy-oriented asymetric supercapacitor but poor electrochemical reversibility.[18]

Commercial symmetric supercapacitors are composed of carbon materials, these devices showed a high power density and an excellent cycling retention, but the energy density based on the device mass (4~6 Wh kg^{-1}) is much lower than batteries and fuel cells, which result in significantly narrow application.[19] As well known, energy density is one of the most important parameters for supercapacitors. To enhance the energy density, carbon materials with electric double capacitance and pseudocapacitive materials with Faradaic capacitance are applied to assemble asymmetric supercapacitors by expanding the electrochemical operation window.[20,21] Nowadays, so many research efforts have been devoted to asymmetric supercapacitor with various materials, such as activated carbon fibre//PANI,[22] AC//MnO_2,[23] vanadium nitride//$Co(OH)_2$,[24] rGO//$Ni(OH)_2$-MnO_2[25] and so on. For example, Tang[26] *et al* reported an asymmetric supercapacitor based on flower-like $Ni(OH)_2$ and activated carbon as anode and cathode, respectively. It showed a maximum specific capacitance of 87.8 F g^{-1} at 0.3 mA and energy density of 32.7 Wh kg^{-1}.

As previously reported, $Ni(OH)_2$/XC-72 composite showed a high specific capacitance of 1560 F g^{-1} at 1 A g^{-1} and good cycling stability with carbon nanotubes as conductive agent.[17] XC-72 is cheaper than AC, but it has better electrical conductivity. The preparation route of $Ni(OH)_2$/XC-72 composite is simple, environmentally friendly and easily

[a] State Key Lab of Oil and Gas Reservoir Geology & Exploitation, Southwest Petroleum University, Chengdu 610500, China. E-mail: spraytang@hotmail.com, Tel/Fax: +86-2883032879
[b] School of Materials Science and Engineering, Southwest Petroleum University, Chengdu 610500, China
[c] School of Chemistry and Chemical Engineering, Southwest Petroleum University, Chengdu 610500, China
[d] Department of Materials Science and Engineering, Norwegian University of Science and Technology, Trondheim 7149, Norway. E-mail: geir.martin.haarberg@ntnu.no, Tel: +47-73594036

scaled-up. Practical application of $Ni(OH)_2$/XC-72 composite in supercapacitor will be considered. In this paper, an AC//$Ni(OH)_2$/XC-72 asymmetric supercapacitor will be assembled and its capacitive performances and cycle life will be studied.

Experimental

Synthesis of $Ni(OH)_2$/XC-72 composite

All solvents and chemicals in this study were used as-received. 60 wt% $Ni(OH)_2$/XC-72 composite was synthesized in a medium of ethylene glycol by a microwave-assisted heating method. The briefly procedure is describedas follows: 20 mg of Vulcan XC-72 was dispersed in 90 mL of ethylene glycol, then 3.2 mL of $NiCl_2$ ethylene glycol solution (0.1 M) was added and stirred for 30 min, later 0.5 M NaOH ethylene glycol solution was added until the pH value reached 11.3, kept continuous agitation for another 30 min. The resulting suspension was heated in a microwave oven (Midea, MM721NH1-PW) with a power of 700 W for 3 min, followed by stirring for 10.5 h to get $Ni(OH)_2$ nanoparticles deposited on carbon black XC-72 at room temperature. Finally, the suspension was filtered, washed by distilled water several times and dried in a vacuum oven at 70°C overnight.

Characterization

The thermal behaviour of the composite was examined by employing Thermogravimetric Analysis (TGA) and Differential Thermal Analysis (DTA) on a TGA/SDTA851^e thermal analyser (Mettler Toledo, Shanghai). The measurements were performed with a heating rate of 10°C min^{-1} from room temperature to 700°C in air. Transmission electron microscopy (TEM) images were taken with a Libra200FE transmission electron microscopy (Carl Zeiss SMT Pte Ltd) operated at 200 kV. The morphology of AC (Fujian Yihuan Carbon Company) was observed on a Zeiss EVO MA 15 scanning electron microscope (SEM).

Fabrication of AC//$Ni(OH)_2$/XC-72 asymmetric supercapacitor devices

The positive electrode was obtained by mixing 60 wt% $Ni(OH)_2$/XC-72 composite, carbon nanotubes (CNTs, Chengdu Organic Chemicals Company, China) and binder (60 wt% Polytetrafluoroethylene (PTFE) emulsion) with a ratio of 85:10:5 in ethanol, then ultrasonically stirred for 30 min, grinded and brushed onto Ni foam (ϕ=14 mm, S=1.54 cm^2) keeping active material loading is 5.5 mg. The obtained electrode is denoted as $Ni(OH)_2$/XC-72/CNT electrode. As for negative electrode, it was obtained by mixing activated carbon (AC), acetylene black and PTFE (60 wt%) with the same mass ratio, procedure and Ni foam diameter as the positive electrode. The mass loading of negative electrode is determined by the mass ratios of cathode to anode. (For example, when the mass ratio of cathode to anode is 1:1, the mass loading of negative electrode is 5.5 mg.) The prepared electrodes dried in vacuum for 6 h before pressed at 10 MPa, followed by immerse in 6 M KOH solution for 18 h to get them fully wetted.

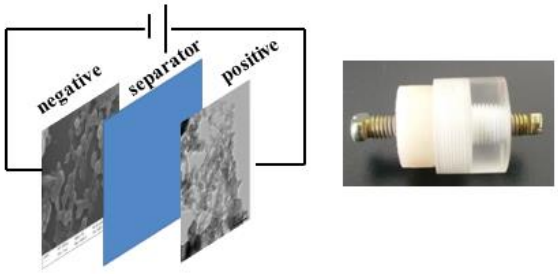

Fig. 1 Schematic of AC//$Ni(OH)_2$/XC-72 asymmetric supercapacitor using $Ni(OH)_2$/XC-72 composite as the positive electrode material, AC as the negative electrode material (Left) and self-made mould (Right) applied for electrochemical testing in a two-electrode system.

The electrodes were separated by glassy fibre membrane (0.2 mm thickness) and non-woven fabric membrane (0.1 mm thickness, ϕ=19 mm, Shenzhen Biyuan Company). The asymmetric supercapacitor was assembled as a sandwich-like configuration in **Fig. 1** (Left) and tested via a self-made mould shown in **Fig.1** (Right).

Electrochemical measurements

Electrochemical performances of an asymmetric supercapacitor were measured by cyclic voltammetry (CV), galvanostatic charge-discharge (GCD) and electrochemical impedance spectroscopy (EIS), using a two-electrode system on an AutoLab Potentiostat 302N (Metrohm Holland). EIS was carried out at open circuit potential and potential amplitude of 5 mV in frequency range of 10^5 Hz to 10^{-2} Hz. Cycling stability was carried out at current density of 10 A g^{-1}. And then, the specific capacitance (F g^{-1}), energy density (Wh kg^{-1}) and power density (W kg^{-1}) were calculated by following equations:

$$C_s = \frac{I\Delta t}{m\Delta V} \quad (1)$$

$$E = \frac{I\int V(t)\mathrm{d}t}{3.6m} \quad (2)$$

$$P = \frac{3600\,E}{t} \quad (3)$$

Where C_s is specific capacitance (F g^{-1}), I is discharging current density (A cm^{-2}), Δt is time (s), ΔV indicates voltage window (V), m is total mass of both two electrodes (g). E and P are energy density (Wh kg^{-1}) and power density (W kg^{-1}), respectively. $\int V(t)\mathrm{d}t$ is integral area of the discharging curve and t is duration of discharging (s).

Results and discussion

Some characterizations like XRD patterns, FT-IR and Raman spectras of $Ni(OH)_2$/XC-72 composite and XC-72 were examined in Ref. 17. Nominal $Ni(OH)_2$ content in the prepared $Ni(OH)_2$/XC-72 composite is 60 wt%, and then the real $Ni(OH)_2$

content will be investigated by TGA. TGA and DTG curves of the $Ni(OH)_2$/XC-72 composite are shown in **Fig. 2**. A total weight loss of 59.5 wt% is observed via three steps as indicated by the zone I, II and III. The weight loss of 6 wt% below 160°C (Zone I) is ascribed to the removal of adsorbed water and evaporation of the intercalated water molecular. [27] The subsequent weight loss of 16.5 wt% (zone II) with a strong peak at 250°C -300°C arises from the loss of water generated by decomposition of $Ni(OH)_2$ to NiO. [28-30] The third zone from 300°C to 540°C with a weight loss of 37 wt% can be ascribed to the burning of carbon material XC-72 in the composite. [31] The residue of ca. 40.5 wt% can be NiO, then $Ni(OH)_2$ content is calculated to be 53.5 wt% in $Ni(OH)_2$/XC-72 composite. This result is in good agreement with nominal 60 wt%.

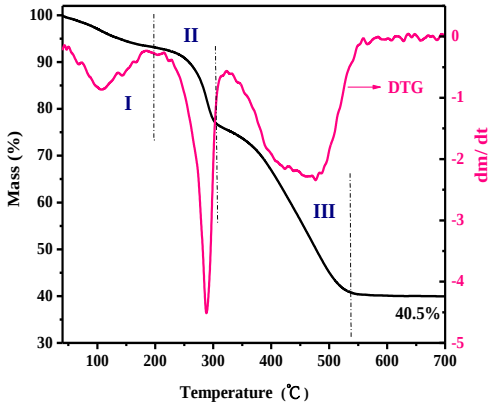

Fig. 2 TGA and DTG curves of $Ni(OH)_2$/XC-72 composite.

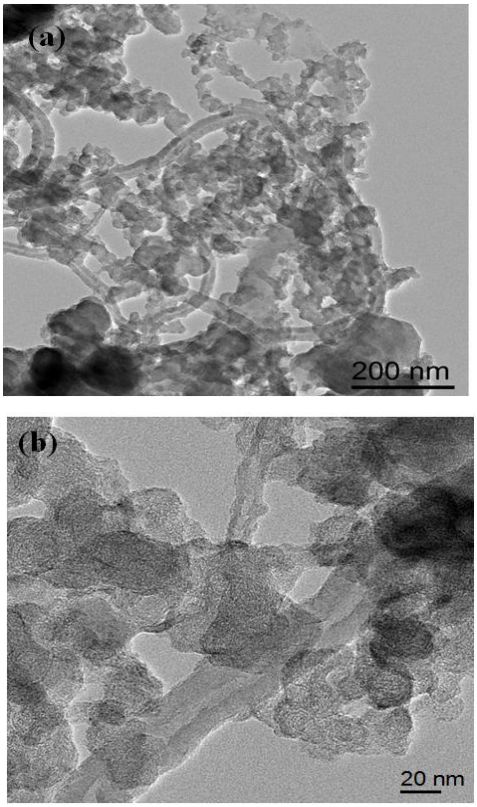

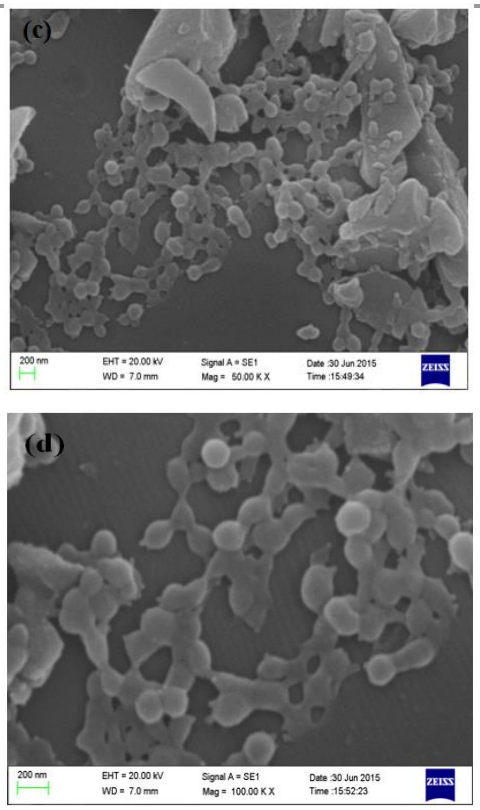

Fig. 3 (a, b) TEM images of $Ni(OH)_2$/XC-72/CNT electrode (c, d) SEM images of activated carbon.

Typical HRTEM images of $Ni(OH)_2$/XC-72/CNT electrode are shown in **Fig. 3**(a, b). It is obviously observed that $Ni(OH)_2$ and XC-72 nanospheres are connected by CNTs to form a three dimensional (3D) conductive network shown in **Fig. 3**(a), and $Ni(OH)_2$ are uniformly distributed onto the surface of XC-72 nanospheres in **Fig. 3**(b). This unique nanostructure will be expected to facilitate the migration of ions and electrons, thus reduces the charging/discharging impedance, and leads to better electrochemical performances. SEM images of AC are displayed in **Fig. 3**(c, d). Activated carbon is composed of interconnected spherical particles, which possesses a large specific surface area (>2100 $m^2\ g^{-1}$). These good properties are benefit for electric double layer energy storage.

Electrochemical performances of AC and $Ni(OH)_2$/XC-72/CNT electrodes

Fig. 4(a) and (b) exhibited CV curves of AC and $Ni(OH)_2$/XC-72/CNT electrode at different scan rates, respectively. It can be seen that a typical shape of EDLC is kept with scan rates from 2 to 20 mV s^{-1} for AC (shown in Fig. 4(a)). The anodic and cathodic potentials are respectively located at 0.41 V and 0.25 V (vs Hg/HgO) for $Ni(OH)_2$/XC-72/CNT elecrode, which reveals a pseudocapacitive behaviour. The redox reaction for $Ni(OH)_2$ is denoted as $Ni(OH)_2 + OH^- \leftrightarrow NiOOH + H_2O + e^-$. GCD curves of AC electrode with different current densities are displayed in **Fig. 4**(c). The shape of the curves at lower current densities is not perfectly like an isosceles triangle, which is caused by the resistance of AC electrode. The specific capacitances are calculated to be 232, 211, 192, 182, 173 F g^{-1} at current

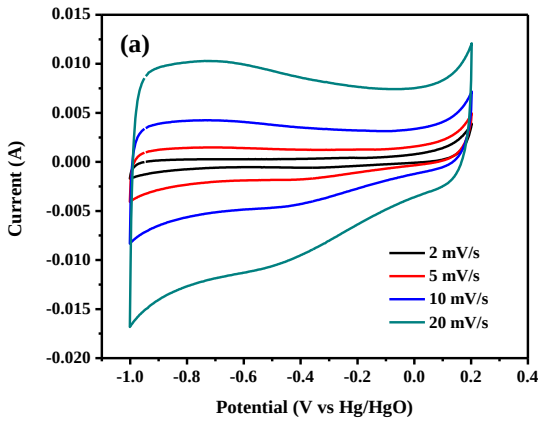

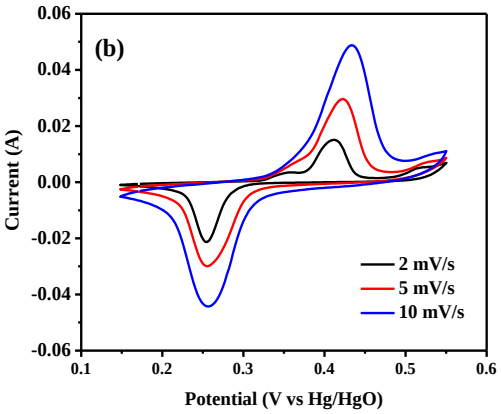

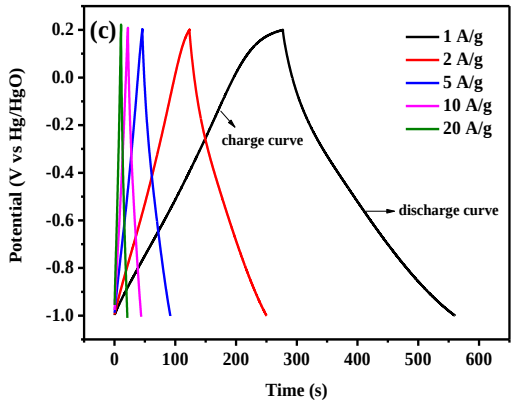

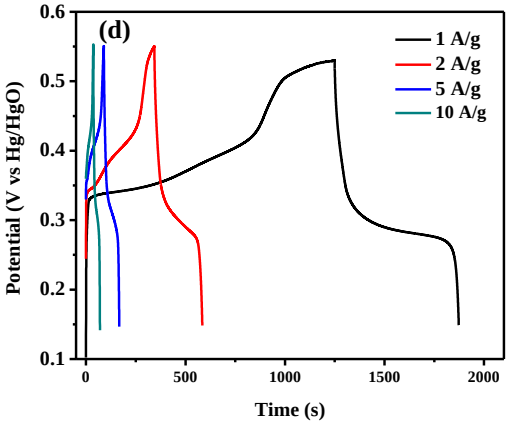

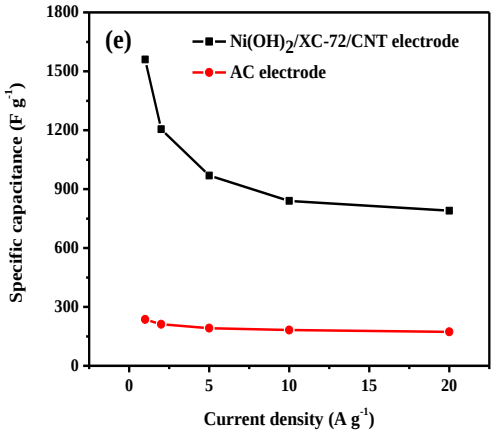

Fig. 4 CV curves of AC (a) and $Ni(OH)_2$/XC-72/CNT electrode (b) at various scan rates; GCD curves of AC (c) and $Ni(OH)_2$/XC-72/CNT electrode (d) at different charging—discharging current densities; (e) specific capacitances of AC and $Ni(OH)_2$/XC-72/CNT tested in a three-electrode system.

densities of 1, 2, 5, 10, 20 A g^{-1} based on eqn. (1) from GCD curves. GCD curves of the $Ni(OH)_2$/XC-72/CNT electrode are shown in **Fig. 4** (d). According to GCD curves and eqn. (1), the specific capacitances are 1560, 1205, 969, 840, 790 F g^{-1} at current densities of 1, 2, 5, 10, 20 A g^{-1}, respectively. The rate capabilities of AC and $Ni(OH)_2$/XC-72/CNT electrodes are shown in **Fig. 4**(e). AC shows excellent rate capability, but the specific capacitance of $Ni(OH)_2$/XC-72/CNT decreases significantly at low discharging current density, then tends to a plateau with increased discharging current densities. Eventually, the specific capacitance of $Ni(OH)_2$/XC-72/CNT is ca. 4.6 times at least of AC.

Asymmetric supercapacitor based on AC//$Ni(OH)_2$/XC-72

The CV curves of AC and $Ni(OH)_2$/XC-72/CNT electrodes tested individually in a three-electrode system at scan rate of 10 mV s^{-1} are shown in **Fig. 5**, which is used to estimate the potential window of the hybrid supercapacitor. For AC, the rectangular-like CV curves in potential range of -1~0.2 V (vs Hg/HgO) indicates the capacitive behaviour of electrode where the charges are stored as electric double layer. For $Ni(OH)_2$/XC-72 composite, the redox peaks are observed in the potential window of 0.15~0.55 V (vs Hg/HgO), which reveals a pseudocapacitive behaviour. There are no other obviously reactions happen from potential of -1.0 V to 0.55 V. Thus, the total cell voltage of the AC//$Ni(OH)_2$/XC-72/CNT asymmetric supercapacitor can be operated close to 1.6 V.

To fabricate AC//$Ni(OH)_2$/XC-72 asymmetric supercapacitors, it is necessary to consider the balance of charges stored in the positive and the negative electrodes.[32,33] Hence, the ideal active material mass ratio of two electrodes can be calculated based on the following equations:

$$q^+ = q^- \quad (4)$$

$$q = C_s \Delta V m \quad (5)$$

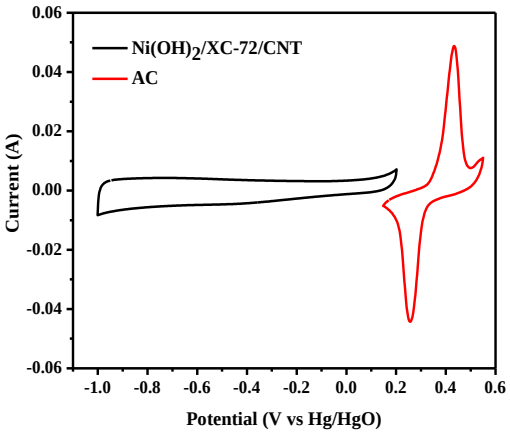

Fig.5 CV curves of AC and $Ni(OH)_2$/XC-72/CNT electrode at scan rate of 10 mV s^{-1}.

$$\frac{m_-}{m_+} = \frac{C_{s+}\Delta V_+}{C_{s-}\Delta V_-} \quad (6)$$

Where C_s is the specific capacitance, ΔV is the potential range during charging-discharging process. In the AC//$Ni(OH)_2$/XC-72 asymmetric supercapacitor system, C_{s+} and C_{s-} are 1560 F g^{-1} with ΔV_+ of 0.4 V and 232 F g^{-1} with ΔV_- of 1.2 V, respectively. Hence, the theoretical m^-/m^+ mass ratio of AC : $Ni(OH)_2$/XC-72 is calculated to be 2.24. However, in a practical asymmetric supercapacitor, the optimum value is usually deviated from the theoretical one. Thus, various active material m^-/m^+ mass ratios of 0.5, 1, 1.25, 1.5, 1.75, 2, 2.25, 2.5, 2.75 and 3 for the negative electrode to the positive were investigated to find out the practically optimal m^-/m^+ mass ratio. Specific capacitance, energy density and power density of the asymmetric capacitors with various m^-/m^+ mass ratios are illustrated in **Table 1**.

Electrochemical performance of AC//$Ni(OH)_2$/XC-72 with various mass ratios of m^-/m^+

Table 1 Specific capacitances, energy densities and power densities of AC//$Ni(OH)_2$/XC-72 asymmetric supercapacitor with various mass ratios using glassy fibre as separator.

Mass ratio of AC : $Ni(OH)_2$/XC-72	Specific capacitance (F g^{-1})	Energy density (Wh kg^{-1})	Power density (W kg^{-1})
0.5	34.1	12.5	412
1	53	22.2	471.5
1.25	60	24.5	460.6
1.5	62.6	24.8	438.4
1.75	69.7	32.3	521.4
2	70	30.8	477.5
2.25	72.6	27.1	435.7
2.5	69.9	27.1	436.3
2.75	45.3	20.4	471.1
3	41.2	18.4	502.7

The specific capacitance of the asymmetric supercapacitor increases with m^-/m^+ mass ratio of AC : $Ni(OH)_2$/XC-72 from 0.5 to 2.25, then decreases from 2.25 to 3. The highest capacitance of 72.6 F g^{-1} with mass ratio of 2.25 is obtained at current density of 0.5 A g^{-1}. For the energy density, its tendency of changing with m^-/m^+ mass ratio is similar to that of the specific capacitance, and a maximum energy density of 32.3 Wh kg^{-1} is achieved when the m^-/m^+ mass ratio is 1.75. As for the power density, it changes with m^-/m^+ mass ratios irregularly, mainly due to an increasing change of the AC amount at the negative electrode. The maximum value of specific capacitance 72.6 F g^{-1} and energy density 32.3 Wh kg^{-1} were obtained, which could be attributed to the charge capacities of $Ni(OH)_2$/XC-72 composite and AC have been correctly matched. When the mass ratio of negative and positive electrode is not matched, it caused their unmatched charge-discharge rates. This charge unbalanced phenomenon reduces the total performances of the asymmetric supercapacitor, including a loss in energyand power density.[32]

The CV curves of AC//$Ni(OH)_2$/XC-72 with mass ratio of 2.25, using glassy fibre as separator, operating at the potential range of 0~1.6 V in a two-electrode system, are shown in **Fig. 6**(a). It exhibits a large current area with a broad redox peak, which is a characteristic of asymmetric supercapacitors containing the electric double layer capacitance and Faradaic pseudo-capacitance, and strong redox peaks are observed from voltage of 0.7 V to 1.6 V, which are much wider than that of positive $Ni(OH)_2$/XC-72 itself. GCD curves at various current

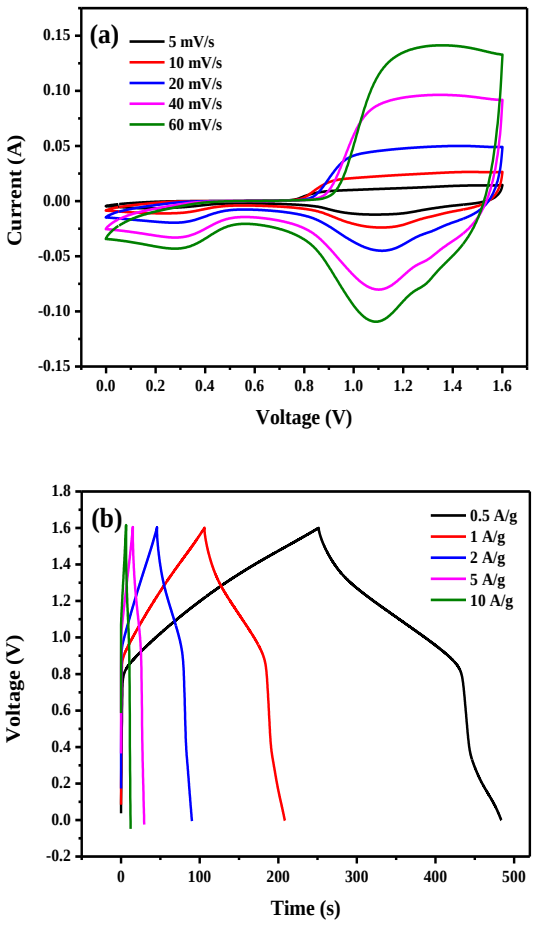

Fig. 6 CV curves at different scan rates (a) and GCD curves at different current densities (b) of the AC//$Ni(OH)_2$/XC-72 asymmetric supercapacitor with mass ratio of 2.25 in two-electrode system and glassy fibre as separator.

densities are displayed in **Fig. 6**(b). The curves are not perfectly symmetry attributed to the electrochemical reversibility of $Ni(OH)_2$/XC-72 composite belonged to battery-like materials.[34] Based on a total mass loading of 17.8 mg for active materials at two electrodes, the specific capacitances of 72.6, 63.9, 55.5, 45.0, 36.3 F g^{-1} were obtained at 0.5, 1, 2, 5, 10 A g^{-1}, respectively.

The influence of different separators to AC//$Ni(OH)_2$/XC-72

As all known, separators are used to prevent the conduction of electrons between two electrodes. It is essential to provide minimal resistance for electrolyte ion's movement and have electronic insulator properties between opposing electrodes.[35] In order to further improve the performances of this asymmetric supercapacitor, non-woven fabric membrane with thickness of 0.1 mm was investigated to as a separator instead of the glassy fibre (0.2 mm). The shapes of CV and GCD curves for AC//$Ni(OH)_2$/XC-72 asymmetric supercapacitor with non-woven fabrics as separator are similar to **Fig.6**(a, b). The specific capacitance, energy density and power density are calculated to be 92.2 F g^{-1}, 36 Wh kg^{-1} and 490.7 W kg^{-1} by eqn. (1-3), respectively. The charging-discharging behaviours at 0.5 A g^{-1} for two different separators are shown in **Fig. 7**(a). The discharging duration of non-woven fabric is 63 s longer than the other one, which may be attributed to the better electrolyte ion's movement. And then, specific capacitances with various current densities are illustrated in **Fig. 7**(b).

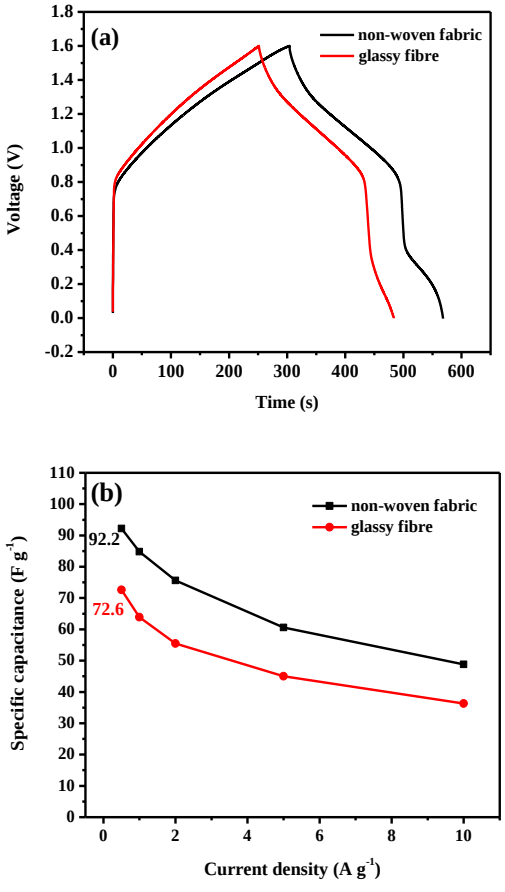

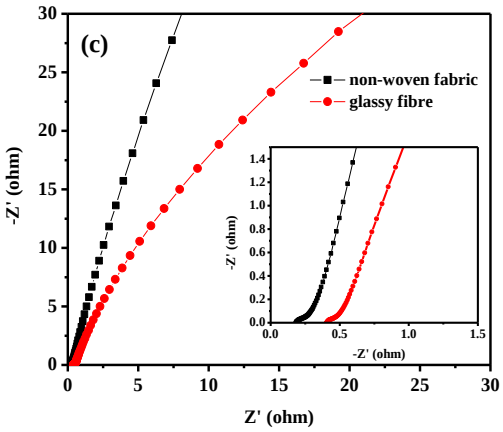

Fig. 7 Comparison of (a) charging-discharging curves at current density of 0.5 A g^{-1} and (b) specific capacitances at different current densities of two separators. (c) Nyquist plots of AC//Ni(OH)2/XC-72 asymmetric supercapacitor with mass ratio of 2.25 using non-woven fibric and glassy fibre as separator, respectively.

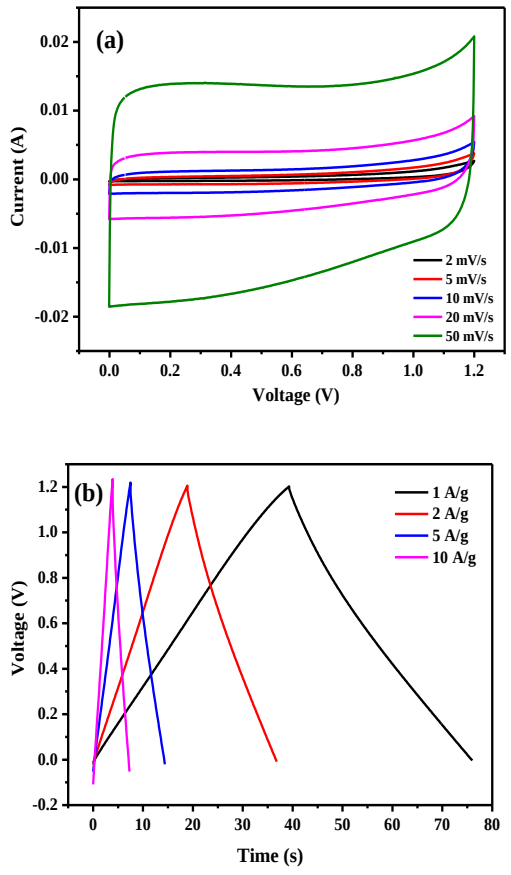

Fig. 8 (a)CV curves at different scan rates and (b) GCD curves at different current densities of AC//AC symmetric supercapacitor with mass loading of 6mg//6mg.

To further explore the resistance of these two separators, EIS measurement was employed to investigate the AC//$Ni(OH)_2$ asymmetric supercapacitor with mass ratio of 2.25 using non-woven fabric and glassy fibre as separator, respectively shown in **Fig. 7**(c). It is obviouly seen that the Rs (0.4 Ω) with glassy fibre as separator is much bigger than the

Table 2 Comparison of AC//$Ni(OH)_2$/XC-72 asymmetric supercapacitor performances with literature data.

Asymmetric supercapacitor	Voltage V	Specific capacitance F g^{-1}	Energy density Wh kg^{-1}	Power density W kg^{-1}	Cycle stability	Reference
AC//Co_2MnO_4/Co	1.5	78	27.8	570.9	98% (10000)	Ref. 4
AC//$Co(OH)_2$/Ni foam	1.6	59.2	20.3	90.6	69% (1000)	Ref. 8
3D rGO//$Ni(OH)_2$	1.7	50	39.9	-	95% (3000)	Ref. 15
AC//$Ni(OH)_2$	1.6	87.8	32.7	71.5	75.3% (1000)	Ref. 26
rGO//$Ni_{0.32}Co_{0.68}(OH)_2$	1.6	-	24	23900	69% (1000)	Ref. 34
GF//CFP@$NiCo_2O_4$	1.6	97.5	34.5	547	92% (10000)	Ref. 36
AC//$Ni(OH)_2$@3D Ni	1.3	92.8	21.8	660	96% (3000)	Ref. 37
AC//$Ni(OH)_2$/XC-72	1.6	92.2	36	490.7	85% (1000)	This work

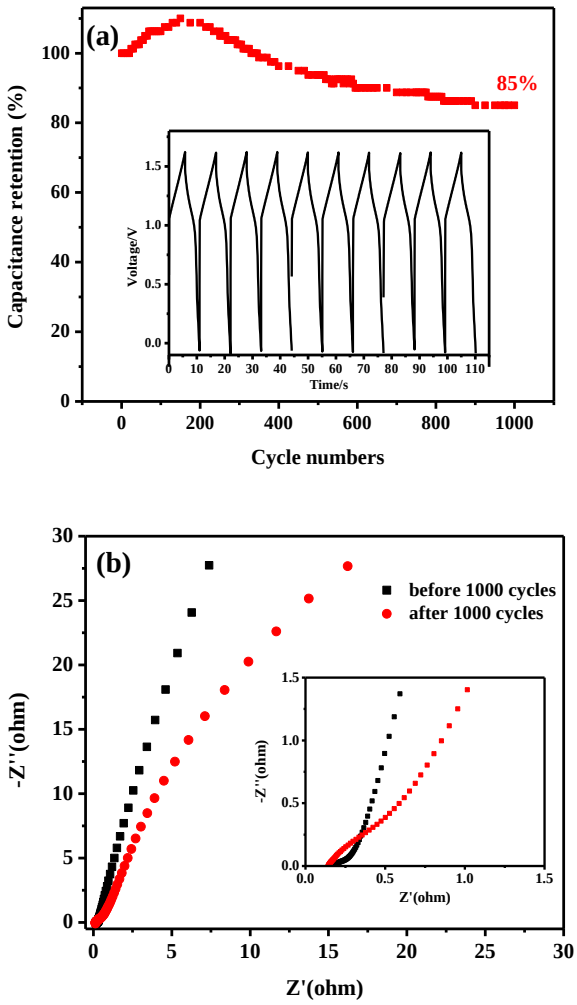

Fig. 9 Cycling performances and EIS of AC// $Ni(OH)_2$/XC-72 asymmetric supercapacitor with mass ratio of 2.25 in 6M KOH electrolyte. (a) Cycle performance at current density of 10 A g^{-1}, inset shows the charge-discharge curves at 10 A g^{-1} (b) Nyquist plots of EIS before and after 1000 cycles, inset shows the impedance at high frequency region.

other one (0.1 Ω). It is clear that the resistance of glassy fibre is higher than non-woven fabric. Therfore, we can draw a conclusion that the electrochemical performance of AC//$Ni(OH)_2$/XC-72 asymmetric supercapacitor with non-woven fabric as separator is much better than glassy fibre.

For comparison, the electrochemical performances of symmetric AC//AC capacitor were also investigated by CV and GCD. The specific capacitance (30.5 F g^{-1} at 1 A g^{-1}) and energy density (6.1 Wh kg^{-1}) are much lower than those of AC//$Ni(OH)_2$/XC-72, as shown in **Fig. 8**(a, b). Furthermore, the performances of the AC//$Ni(OH)_2$/XC-72 asymmetric supercapacitor are compared with the reported AC//Co_2MnO_4/Co[4], AC//$Co(OH)_2$/Ni foam,[8] 3D rGO//$Ni(OH)_2$,[15] AC//$Ni(OH)_2$,[26] rGO//$Ni_{0.32}Co_{0.68}(OH)_2$,[34] GF//CFP@$NiCo_2O_4$,[36] AC//$Ni(OH)_2$@3D Ni,[37] AC//(Ni-Co-Cu)$(OH)_2$-CuO,[38] supercapacitors in recent years, as illustrated in **Table 2**. The performances of this asymmetric supercapacitor are better than or comparable to those reported data, which can be ascribed to the unique 3D conductive nanostructure of $Ni(OH)_2$/XC-72/CNT electrode and good EDLC capacitive behaviour of AC.

Excellent cycle stability is another crucial requirement for practical applications of supercapacitors. The cycling life of the AC//$Ni(OH)_2$/XC-72 asymmetric supercapacitor was carried out by galvanostatic charge-discharge at a current density of 10 A g^{-1} between 0~1.6 V for 1000 cycles, as illustrated in **Fig. 9**(a). The asymmetric capacitor maintains 85% of its initial capacitance (78.4 F g^{-1}) after 1000 cycles, which is comparable to reported nickel or cobalt based capacitor.[6,8,25] It is noticed that the capacitance retention increases ca. 10% during initial 150 cycles, mainly thanks to an electro-activation process of electrode materials.[39-41] The subsequent decrease might be ascribed to the increased charge transfer resistance and diffusion resistance after the cycling. The asymmetric capacitor possesses an acceptable cycle stability performance.

The electrochemical impedance spectroscopy (EIS) is a powerful technique to evaluate the reaction mechanism in electrochemical system, herein it is employed to investigate the reaction change of the AC//$Ni(OH)_2$/XC-72 asymmetric supercapacitor before and after the 1000-cycle GCD tests. The Nyquist plots are shown in **Fig. 9**(b). There is no change for real resistance (R_s) before and after life tests, Rs maintains at 0.18 Ω. For charge-transfer resistance (R_{ct}), it increases from tiny resistance of 0.1 Ω to 0.3 Ω after cycling experiment, this could be due to agglomeration of $Ni(OH)_2$ nanoparticles. Before life test, the diffusion behaviour is more close to that of an EDLC, presents a nearly vertical line, representing the capacitive-like responses. This phebomenon indicate a high capacitive behaviour and ion diffusion on the structure of the nanomaterial.[42,43] After 1000-cycle GCD test, the diffusion line is more close to the line with slop of π/4, results in the decay of electrochemical performances.

Conclusions

$Ni(OH)_2$/XC-72 composite can be prepared by microwave assisted method, with small $Ni(OH)_2$ nanoparticles uniformly distributed on the surface pf XC-72, which displayed a high specific capacitance of 1560 F g^{-1} at current density of 1 A g^{-1} as electrode material. The AC//$Ni(OH)_2$/XC-72 asymmetric supercapacitor exhibits an energy density of 36 Wh kg^{-1} and power density of 490 W kg^{-1} based on active material in 6 M aqueous electrolyte using non-woven fabric as separator. Furthermore, the maximum specific capacitance of 92.2 F g^{-1} with total mass loading of 17.8 mg can be achieved at current density of 0.5 A g^{-1} within a voltage window of 1.6 V, and the capacitance retention maintains 85% after 1000 galvanostatic charging-discharging cycles. Therefore, the AC//$Ni(OH)_2$/XC-72 supercapacitor is promising to be applied in a practical device for energy storage.

Acknowledgements

This work was supported by Scientific Research Foundation for Returned Scholars, Ministry of Education of China, International Technology Collaboration of Chengdu Science and Technology Division, the Open Project from State Key Lab of Catalysis (N-14-1), the Technology Project of Education Department of Sichuan Province (13ZA0193).

References

1. Q. Li, Z. L. Wang, G. R. Li, R. Guo, L. X. Ding and Y. X. Tong, Nano Lett., 2012, 12, 3803-3807.
2. M. F. El-Kady, V. Strong, S. Dubin and R. B. Kaner, Science, 2012, 335, 1326-1330.
3. P. Simon and Y. Gogotsi, Nat. Mater., 2008, 7, 845-854.
4. M. J. Jing, H. S. Hou, Y. C. Yang, Y. R. Zhu, Z. B. Wu and X. B. Ji, Electrochim. Acta, 2015, 165, 198-205.
5. Q. Q. Tang, M. M .Chen, L. Wang, G. C. Wang, J. Power Sources, 2015, 273, 654-662.
6. W. W. Liu, X. Li, M. H. Zhu and X. He, J. Power Sources, 2015, 282, 179-186.
7. X. Y. Cai, S. H. Lim, C. K. Poh, L. F. Lai, J. Y. Lin and Z. X. Shen, J. Power Sources, 2015, 275, 298-304.
8. S. Yang, K. Cheng, K. Ye, Y. J. Li, J. Qu, J. L. Yin, G. L. Wang and D. X. Cao, J. Electroanal. Chem., 2015, 741, 93-99
9. P. M. Kharade, S. G. Chavan,D. J. Salunkhe, P. B. Joshi, S. M. Mane and S. B. Kulkarni, Mater. Res. Bull., 2014, 52, 37-41.
10. X. Y. Cai, S. H. Lim, C. K. Poh, L. F. Lai, J. Y. Lin and Z. X. Shen, J. Power Sources, 2015, 275, 298-304.
11. G. F. Chen, Z. Q. Liu, J. M. Lin, N. Li and Y. Z. Su, J. Power Sources, 2015, 283, 484-493.
12. G. F. Chen, Y. Z. Su, P. Y. Kuang, Z. Q. Liu, D. Y. Chen, X. Wu, N. Li and S. Z. Qiao, Chem. Eur. J., 2015, 21, 4614-4621.
13. C. C. Hu, K. H. Chang, M. C. Lin and Y. T. Wu, Nano Lett. , 2006, 6: 2690-2695.
14. Y. Zhang, C. Sun, P. Lu, K. Y. Li, S. Y. Song and D. F. Xue, CrystEngComm. 2012, 14, 5892-5897.
15. F. Luan, G. M. Wang, Y. C. Ling, X. H. Lu, H. Y. Wang, Y. X. Liu and Y. Li, Nanoscale, 2013, 5, 7984-7990.
16. Y. Hou, L.Y. Chen, P. Liu, J. L. Kang, T. S. Fujita and M. W. Chen, J. Mater. Chem. A, 2014, 2, 10910-10916.
17. S. H. Tang, L. P. Sui, Z. Dai, Z. T. Zhu and H. X. Huangfu, RSC Adv., 2015, 5, 43164-43171.
18. C. C. Hu, J. C. Chen and K. H. Chang. J. Power Sources, 2013, 221, 128-133.
19. C. F. Zhou, S. Kumar, C. D. Doyle and J. M. Tour, Chem. Mater., 2005, 17, 1997-2002.
20. X. Xiao, T. P. Ding,L.Y. Yuan, Y. Q. Shen, Q. Zhong, X. Zhang, Y. Z. Cao, B. Hu, T. Zhai, L. Gong, J. Chen, Y. Tong, J. Zhou and Z. L. Wang, Adv. Energy Mater., 2012, 2, 1328-1332.
21. X. H. Lu, M. H. Yu, G. M. Wang, T. Zhao, S. L. Xie, Y. C. Ling, Y. X. Tong and Y. Li, Adv. Mater., 2013, 25, 267-272.
22. D. S.Torres, J. M. Sieben,D. Lozano, D. C. Amoros and E. Morallon, Electrochim. Acta, 2013, 89, 326-333.
23. J. Yang, L. F. Lian,H. C. Ruan, F. Y. Xie and M. D. Wei, Electrochim. Acta, 2014, 136, 189-194.
24. R. T. Wang, X. B. Yan, J. W. Lang, Z. M. Zhang and P. Zhang, J. Mater. Chem. A, 2014, 2, 12724-12732.
25. H. Chen, L. F. Hu, Y. Yan, R. C. Chen, M. Chen and L. M. Wu, Adv. Energy Mater., 2013, 3, 1636-1646.
26. Y. F. Tang, Y. Y. Liu, S. G. Yu, Y. F. Zhao, S. C. Mu and F. M.Gao, Electrochim. Acta, 2014, 123, 158-166.
27. L. Qian, L. Gu, L. Yang, H. Y. Yuan and D. Xiao, Nanoscale, 2013, 5, 7388-7396.
28. J. Xiao and S. Yang, RSC Adv., 2011, 1, 588-595.
29. S. J. Guo, S. J. Dong and E. Wang, ACS Nano., 2010, 4, 547-555.
30. D. B. Kuang, B. X. Lei, Y. P. Pan, X. Y. Yu and C. Y.Su, J. Phys. Chem. C, 2009, 113, 5508-5513.
31. H. J. Yan, J. W. Bai, J. Wang, X. Y. Zhang, B. Wang, Q. Liu and L. H. Lin, Cryst. Eng. Comm., 2013, 15, 10007-10015.
32. C. C. Hsu, C. C. Hu, T. H. Wu, J. C. Chen and M. Rajkumar. Electrochim. Acta, 2014, 146, 759-768.
33. Z. Fan, J. Yan, T. Wei, L.J. Zhi, G. Q. Ning, T. Y. Li and F. Wei, Adv. Funct. Mater., 2011, 21, 2366-2375.
34. J. C. Chen, C. T. Hsu and C. C. Hu, J. Power Sources, 2014, 253, 205-213.
35. H. J. Yu, Q. W. Tang, J. H. Wu, Y. Z. Lin, L. Q. Fan, M. L. Huang, J. M. Lin, Y. Li and F. D. Yu, J. Power Sources, 2012, 206, 463-468.
36. Q. Q. Tang, M .M. Chen, L.Wang and G.C. Wang J. Power Sources, 2015, 273, 654-662.
37. Y. Z. Su, K. Xiao, N. Li, Z. Q. Liu and S. Z. Qiao, J. Mate. Chem. A, 2014, 2, 13845-13853.
38. C. H. Lien, C. C.Hu, C. T. Hsu and D. S. Wong, Electrochemi. Commun. 2013, 34, 323-326.
39. C. C. Hu, K. H. Chang and T. Y. Hsu, J. Electrochem. Soc., 2008, 155, F196- F200.
40. C. C. Hu, C. T. Hsu, K. H. Chan and H. Y. Hsu, J. Power Sources, 2013, 238, 180-189.
41. C. T. Hsu, C. C. Hu, J. Power Sources, 2013, 242, 662-671.
42. J. Kang, J. Wen, S. H. Jayaram, X. H.Wang and S. K.Chen, J. Power Sources, 2013, 234, 208-216.
43. Q. Cheng, J. Tang, N. Shinya and L. C. Qin, J. Power Sources, 2013, 241, 423-428.

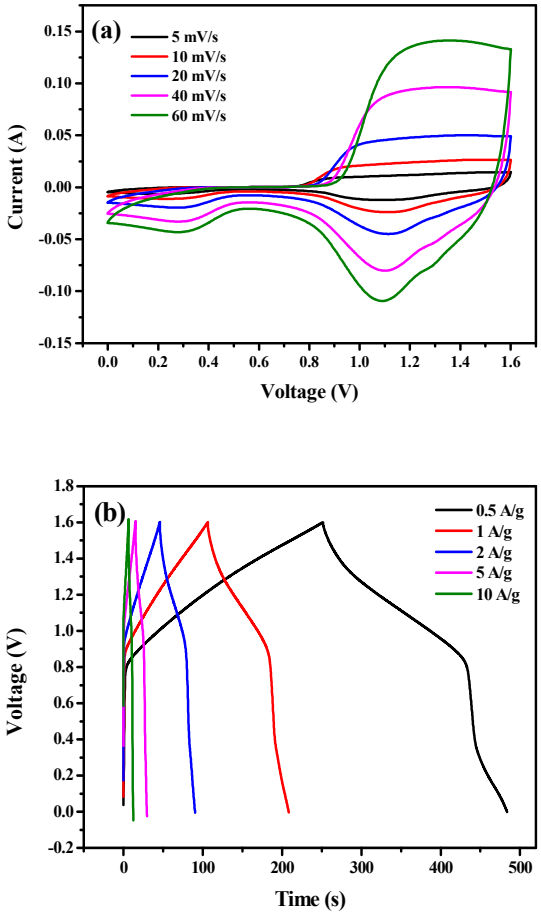

AC//Ni(OH)$_2$/XC-72 asymmetric supercapacitor with non-woven fabrics based on active material exhibited the superior electrochemical performance.